Preparing Reagents: Time Dependence of HCl(v = 1, J) Alignment Following Pulsed Infrared Excitation

A.J. Orr-Ewing,* W.R. Simpson, T.P. Rakitzis, and R.N. Zare†
Department of Chemistry, Stanford University, Stanford, California 94305, USA

(Received 2 November 1993)

Abstract. We discuss the use of photon absorption as a means of aligning reagents for studies of dynamical stereochemistry. A linearly polarized infrared beam from an optical parametric oscillator prepares HCl(v = 1, J = 1), and the alignment is monitored at subsequent times by (2+1) resonance-enhanced multiphoton ionization. The degree of alignment oscillates in time caused by hyperfine quantum beats. Experimental observations are well matched by calculations that account for the presence of unresolved hyperfine structure. Following reagent preparation by optical pumping, a cumulative hyperfine-depolarization coefficient can be used to describe the effective reagent alignment in a subsequent chemical reaction.

1. INTRODUCTION

Several experimental strategies have been employed to collide oriented or aligned reagents with a directional beam of a second reagent (typically an atomic species),[1–8] or to orient reagents using intermolecular forces[9–12] to study the angular requirements for reaction. For oriented molecules, two ends of the molecule can be distinguished; for reaction of, for example, BC with A, the B or C end of the molecule can be directed toward A. For an aligned reagent, the only distinction possible is between the end or the side of the molecule, so attack by A at either B or C can be differentiated from side-on attack, but attack at B cannot be separated from attack at C.[13]

One promising approach for preparing aligned reagents is to use optical pumping techniques[14] because the use of linearly polarized light leads naturally to aligned samples.[1,13,15–20] One-photon absorption has been used, for example, to align HF with respect to a beam of Sr atoms or Li atoms.[6, 7, 21] Early results for the Sr + HF reaction that showed a reagent-alignment dependence to the SrF product quantum-state population distribution could not be reproduced,[22] but a strong dependence of product angular distributions, the partitioning of available energy, and reaction cross sections on the reagent alignment were found for the Li + HF(v = 1) reaction.[7] Kettleborough and McKendrick[23] calculated the extent to which prepared alignment is lost because of thermal motion of an optically-pumped gas in beam-gas experiments. Elastic M-changing collisions of $H_2(B^1\Sigma_u^+, v = 0, J = 1, M = 0)$ with He, Ne, Ar, and $H_2(X^1\Sigma_g^+)$ were studied by Pibel and Moore,[24] using one-photon absorption on an R(0) transition to prepare the aligned H_2 in the B state. Stimulated Raman pumping (SRP) was used by Sitz and Farrow[25] to prepare N_2 rotationally aligned in a vibrationally-excited state, and Dopheide and Zacharias[26] recently used SRP to align acetylene.

Experiments that employ optical excitation to prepare aligned reagents are prone to depolarization of the alignment because of the coupling of the rotational angular momentum of the molecular framework, **J**, to external fields, the spin(s) of the nuclei (hyperfine coupling), or to the spins of the electrons for open-shell molecules.[27–32] In the study of bimolecular reactions, such depolarization effects can significantly alter the alignment or orientation of prepared reagents because, in general, reaction will not occur immediately upon preparation of the reagents. Likewise, the nascent polarization of **J'** for reaction products will be affected by coupling to external fields or intramolecular spin angular momenta during the time delay between reaction and detection. In this paper, we focus on nuclear-spin hyperfine-depolarization effects but note that such considerations apply to molecules with nonzero electronic spin. In such cases of net electronic spin, we can describe the depolarization of the total

*Present address: School of Chemistry, University of Bristol, Cantock's Close, Bristol BS8 1TS, UK.
†Author to whom correspondence should be addressed.

angular momentum excluding spin, **N**, caused by coupling to the electronic spin, **S**, to give a resultant total angular momentum **J**.

We can understand the depolarization of **J** in terms of the vector model of angular momenta; **J** couples to the nuclear spin, **I**, to give **F**, and then **J** precesses about **F** so that the prepared direction of **J** in space is lost to some extent. The degree to which the alignment is depolarized depends both on the strength of the coupling and on the relative magnitudes of **J** and **I**. For values of **J** substantially larger than the magnitude of **I** (typically **I** takes values up to about 5/2 for a single nuclear spin) **J** and **F** will be nearly parallel, and the hyperfine depolarization will be small. For magnitudes of **J** close to or smaller than those of **I**, hyperfine depolarization can severely reduce the degree of orientation or alignment. The timescale for the hyperfine depolarization depends on the strength of the coupling between **J** and **I**, or, in the vector model, on the rate of precession of **J** about **F**.

We prefer to discuss the hyperfine depolarization in terms of quantum beats.[33–35] If the coherent bandwidth of the excitation laser is greater than the splittings of the rotational level caused by coupling of **J** to the nuclear spin, we create a coherent superposition of hyperfine sublevels when we drive the absorption step with our laser. This coherent superposition of states will evolve in time; if we probe the excited state at different times after the excitation pulse, we will observe beating between the coherently excited sublevels. The most apparent consequence of this time evolution will be a dephasing of the initially prepared alignment. If we were to use a laser of sufficiently narrow bandwidth that we could excite just one hyperfine sublevel, the prepared alignment would display no time dependence. The experiment we describe in this paper makes use of a laser with bandwidth sufficient to prepare a coherent superposition of hyperfine sublevels, and therefore is an example of the infrequently studied phenomenon of quantum beats within the ground electronic state of a molecule.[36–38]

2. EXPERIMENTAL APPARATUS

The apparatus used in the experiments has been described in detail elsewhere.[39] In brief, HCl REMPI detection was performed in a linear time-of-flight mass-spectrometer comprising two differentially pumped chambers. The ions formed in the first chamber were extracted through a slit into a field-free flight tube and were subsequently detected using chevron-configuration microchannel plates (Galileo). HCl, diluted to less than 1% in helium to make a total pressure of 500 Torr, was injected into the first chamber through a pulsed valve. The contamination of HCl($v = 1$) in the gas mixture downstream from the nozzle was negligible. The HCl was aligned by infrared excitation using the output of a lithium niobate optical parametric oscillator (OPO) which was pumped by a Nd:YAG laser (Spectra Physics DCR-1). Excitation was performed at 2906 cm^{-1} on the R(0) transition of the fundamental vibrational transition of ground-state HCl, and the OPO bandwidth was ca. 1 cm^{-1}. The coherent IR beam was linearly polarized, and a photoelastic modulator (Hinds, PEM-80) placed in the beam path was used to change the linear polarization of the IR beam between horizontal and vertical on a shot-to-shot basis. After a variable time delay, a probe laser operating at ca. 249.9 nm ionized the HCl($v = 1, J = 1$) via a (2+1) REMPI scheme through the $F^1\Delta$ Rydberg state. We used the output of a Nd:YAG-pumped dye laser (Spectra Physics DCR-2AG and PDL-3) operating on LD 489 laser dye (Exciton) and frequency doubled in a β-barium borate (BBO) crystal to generate the 249.9-nm laser beam. The HCl^+ ions were collected without discrimination against any velocity group.

Data were also recorded for an angle between the polarizations of the excitation and probe beams of 54.7 ° (the magic angle, see section 3). This configuration of polarizations was achieved by fixing the OPO polarization and inserting a half-wave plate and polarizer in the probe laser beam path.

The timing between the excitation and probe pulses was controlled by a delay generator (Stanford Research Systems DG535). The convolution of the probe laser and OPO pulse widths with the residual jitter in the trigger timing resulted in an effective time resolution of 14 ns. This time resolution was confirmed by differentiating the rising edge of the REMPI signal recorded under conditions where no observable oscillation occurred caused by hyperfine depolarization (at the magic angle). The probe laser operated at a frequency of 20 Hz, whereas the OPO operated at a 10 Hz repetition rate, thereby allowing a shot-by-shot subtraction of background signal that was not induced by the IR beam.

3. RESULTS

Figure 1 presents experimental data for the (2+1) REMPI signal intensity, recorded on the R(1) line of the HCl $F^1\Delta$-$X^1\Sigma^+(0,1)$ transition as a function of the time delay between the OPO excitation pulse and the probe laser pulse. Each point represents a 160-shot sum of data recorded over a 4-ns time window. In this figure, we show data for the OPO polarization parallel and perpendicular to the linear polarization of the probe laser and for a magic angle of 54.7° between the excitation and probe polarizations. IR absorption from the vibrational ground state of HCl and from an initial rotational state J_i to the first vibrationally-excited state with rotational quantum number J aligns the HCl($v = 1, J$). For R(0) excitation, $J_i = 0$ and $J = 1$. The ion-signal intensity is related to the alignment of the HCl($v = 1, J = 1$) by an expression of the form:[40]

$$I = C\{P_0^{(0)}(J, J_f;\theta)\, A_0^{(0)}(J) + P_0^{(2)}(J, J_f;\theta)\, A_0^{(2)}(J)\} \quad (1)$$

where C is a constant that includes such factors as the

laser-beam intensities and the detector efficiency, and the $A_0^{(k)}(J)$ terms are alignment parameters (with $A_0^{(0)}(J)$ normalized to unity). J_f is the rotational quantum number of the state accessed by the two-photon absorption, and the $P_0^{(k)}(J, J_f; \theta)$ factors are termed the line-strength moments. These line-strength moments contain all the terms involving the angular-momentum coupling for the two-photon transition used to probe the HCl and the dependence of the signal on the angle, θ, between the excitation and probe laser polarizations. Thus, the oscillations observed in the signal intensity with time are a consequence of the oscillatory depolarization of the second (or quadrupolar) alignment moment, $A_0^{(2)}(J)$ as discussed in the following section. The oscillations vanish when $\theta = 54.7°$ because at this magic angle, the second-order line-strength moment, $P_0^{(2)}(J, J_f; 54.7°) = 0$. At the magic angle, a measurement of the signal intensity is directly proportional to the population of the HCl($v = 1$) in the rotational state with quantum number J.

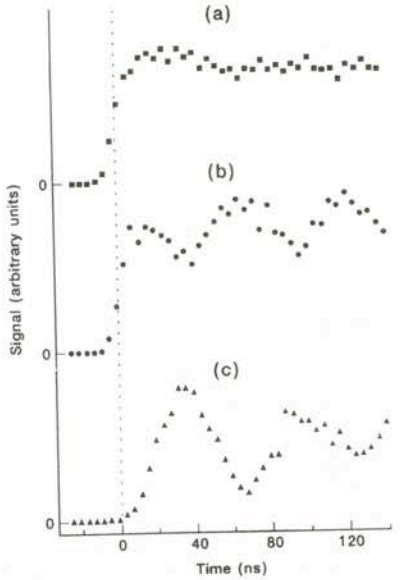

Fig. 1. HCl^+ ion signal detected by (2+1) REMPI on the R(1) line of the HCl $F^1\Delta$-$X^1\Sigma^+(0,1)$ two-photon transition as a function of the time delay between the excitation and probe pulses. The excitation beam is linearly polarized and excites HCl to $v = 1$, $J = 1$ on the R(0) line, preparing an aligned sample. The figure shows data sets for three different angles, θ, between the electric vectors of the linearly polarized excitation and probe beams: (a) $\theta = 54.7°$ (the magic angle), (b) $\theta = 90°$, and (c) $\theta = 0°$. At the magic angle (a), only the population is probed, whereas (b) and (c) are sensitive to the rotational alignment of the HCl($v = 1, J = 1$) molecules. The oscillations of the signal intensity with time are a consequence of the hyperfine depolarization of the rotational alignment. Data sets (b) and (c) were recorded using polarization switching on an every-other-shot basis, as described in the text, and thus their magnitudes and time axes are related absolutely. The vertical dotted line marks the point where the peaks of the excitation and probe pulses are coincident in time. At this time delay of zero, data set (c) has no intensity, whereas data set (b) shows a rising signal. This observation of no HCl REMPI signal for coincident pulses with parallel polarizations is discussed in section 4.1 of the text. Data set (a) was recorded in a separate experiment and thus has been scaled and shifted in time to be displayed on the same axes.

4. DISCUSSION

4.1 Calculation of Hyperfine Depolarization

The general expression for the excited-state density matrix following one-photon, unsaturated absorption from a state $|J_i M_i\rangle$ to a state $|JM\rangle$ is well known:

$$\langle JM|\rho|JM\rangle_{IR} \propto |\langle J\|r^{(1)}\|J_i\rangle|^2 \sum_{M_i} \begin{pmatrix} J & 1 & J_i \\ -M & \mu_0 & M_i \end{pmatrix}^2 \qquad (2)$$

Here, the subscript *IR* denotes density-matrix elements in the excitation frame, (:::) is a Wigner 3-j symbol, and μ_0 is the projection of the photon angular momentum onto the excitation-frame symmetry axis ($\mu_0 = 0$ for linearly polarized light, and $\mu_0 = \pm 1$ for circularly polarized light). The reduced-matrix-element term is related to the transition line strength. The azimuthal symmetry about the linear-polarization vector, $\mathbf{E}_{IR}$, or about the beam propagation axis for circular polarization, causes nondiagonal density-matrix elements to vanish.

The degree of alignment of the excited state at the instant of photon absorption can be calculated by writing the density matrix of eq 2 in terms of state-multipole moments,[29] which in turn can be related to alignment parameters.[13] $R(0)$ excitation of HCl with linearly polarized light produces a highly aligned sample because in the unsaturated regime, the $\Delta M = 0$ selection rule restricts production of HCl($v = 1$, $J = 1$) to the single magnetic sublevel $M = 0$ in the frame of the polarization of the IR beam. This M-state population distribution corresponds to a quadrupolar alignment parameter $A_0^{(2)} = -1$, and apart from the monopolar parameter, $A_0^{(0)} = +1$, all other orientation and alignment parameters in the frame of $\mathbf{E}_{IR}$ are zero. One consequence of this high degree of quadrupolar alignment is apparent in Fig. 1, where for coincident excitation and probe pulses ($t = 0$), no HCl REMPI signal intensity is observed for the parallel configuration of the IR and probe beam polarizations. For the perpendicular configuration, signal is observed for coincident pulses. This lack of REMPI intensity at $t = 0$ in Fig. 1c can be understood from eq 1. For detection via the $R(1)$ transition, the calculated line-strength moments are $P_0^{(2)}(J = 1, J_f = 2, \theta = 0°) = 1$ and $P_0^{(2)}(J = 1, J_f = 2, \theta = 90°) = -\frac{1}{2}$, with the normalization that $P_0^{(0)}(J, J_f, \theta) = 1$. Thus, for $A_0^{(0)} = +1$ and $A_0^{(2)} = -1$, the REMPI signal intensity vanishes for $\theta = 0°$ because the zeroth- and second-order

terms in eq 1 cancel. In Fig. 1c, signal intensity grows as the time delay between the excitation and probe pulses increases from zero. During this elapsed time the magnitude of the quadrupolar alignment decreases because of hyperfine depolarization.

We make the assumptions that (i) at the instant of formation of molecules in an aligned or oriented ensemble by optical pumping, the rotational angular momentum is uncoupled from the nuclear-spin angular momenta, but that the different momenta then couple to give a resultant, **F**, and (ii) the nuclear spins are unpolarized at the instant of optical pumping. Yan and Kummel[32] discussed the effect of hyperfine coupling on the degree of alignment of reagents created by photodissociation. Their considerations were restricted to the long-time limit, however, because of their interest in scattering aligned molecules from surfaces (we note that these authors' calculations of hyperfine-depolarization coefficients for Cl_2 erroneously used a value for the Cl-atom nuclear spin of 5/2 and this error also arises in ref 41). For experiments in which the reagents are aligned by optical excitation and reaction follows on a timescale that is typically submicrosecond, such as for photolysis-induced reactions of translationally hot atoms under bulb conditions,[42] we must take into account the time dependence of the hyperfine coupling.[31] The time-dependent and long-time-average depolarization effects are summarized below.

Derivations of the hyperfine-depolarization results for a molecule with a single nuclear spin are given in terms of a state-multipole treatment by Blum,[29] and in terms of a spherical-tensor-operator treatment by Zare.[30] If the rotational-angular-momentum distribution at the instant of formation of the oriented or aligned ensemble (time, $t = 0$) is described by a set of orientation and alignment parameters,[13] $A_q^{(k)}(J;t=0)$, then at some later time t, the parameters are given by:

$$A_q^{(k)}(J;t) = G^{(k)}(t) A_q^{(k)}(J;t=0) \tag{3}$$

where $G^{(k)}(t)$ is a time-dependent depolarization coefficient:

$$G^{(k)}(t) = \sum_{F,F'} \frac{(2F'+1)(2F+1)}{(2I+1)} \begin{Bmatrix} F' & F & k \\ J & J & I \end{Bmatrix}^2 \times \cos[(E_{F'} - E_F)t/\hbar] \tag{4}$$

In this equation, the E_F are the eigenvalues of the hyperfine Hamiltonian, i.e., they are the energy levels arising from the coupling of the rotational and nuclear spin angular momenta. They can be calculated from hyperfine coupling constants. Note that the interaction between **J** and **I** does not mix multipole moments of **J**, but it does result in a decrease in their values over time. The function $G^{(k)}(t)$ is oscillatory and seldom returns to its original value of unity. The time-averaged value of $G^{(k)}(t)$ is useful for measurements made on a timescale longer than the oscillation period of $G^{(k)}(t)$ and is given by:

$$\langle G^{(k)} \rangle = \frac{1}{(2I+1)} \sum_F (2F+1)^2 \begin{Bmatrix} F & F & k \\ J & J & I \end{Bmatrix}^2 \tag{5}$$

Fano and Macek[28] discussed the effect of the coupling of two spins, and Altkorn, Greene, and Zare[31, 43] derived an expression for the depolarization coefficient for depolarization by two nuclear spins, $\mathbf{I}_1$ and $\mathbf{I}_2$:

$$G^{(k)}(t) = \frac{1}{(2I_1+1)(2I_2+1)} \sum_{\substack{\alpha,\alpha' \\ F,F'}} (2F'+1)(2F+1) \times \left| \sum_{F_i,F_i'} (-1)^{F_i+F_i'} [(2F_i+1)(2F_i'+1)]^{1/2} \times c_{\alpha F_i}^{(F)} c_{\alpha' F_i'}^{(F')*} \begin{Bmatrix} F_i' & F' & I_2 \\ F & F_i & k \end{Bmatrix} \begin{Bmatrix} J & F_i' & I_1 \\ F_i & J & k \end{Bmatrix} \right|^2 \times \cos[(E_{\alpha F} - E_{\alpha' F'})t/\hbar] \tag{6}$$

which has a long-time-averaged form:

$$\langle G^{(k)} \rangle = \frac{1}{(2I_1+1)(2I_2+1)} \sum_{\alpha,F} (2F+1)^2 \times \left| \sum_{F_i,F_i'} (-1)^{F_i+F_i'} [(2F_i+1)(2F_i'+1)]^{1/2} \times c_{\alpha F_i}^{(F)} c_{\alpha' F_i'}^{(F')*} \begin{Bmatrix} F_i' & F' & I_2 \\ F & F_i & k \end{Bmatrix} \begin{Bmatrix} J & F_i' & I_1 \\ F_i & J & k \end{Bmatrix} \right|^2 \tag{7}$$

In a hierarchical-coupling scheme, **J** and $\mathbf{I}_1$ couple together to give $\mathbf{F}_i$, and $\mathbf{F}_i$ subsequently couples to $\mathbf{I}_2$ to give the total angular momentum, **F**. In the limit of a hierarchical-coupling scheme, F_i is a good quantum number. When such α hierarchical-coupling scheme is not applicable, α replaces F_i as an intermediate quantum number. Assigning particular values to α is not necessary because they serve only as labels to differentiate between states. The states that diagonalize the hyperfine Hamiltonian are labeled by F and α in this instance. The nonhierarchical basis can be expanded in hierarchical-coupling wave functions thus:

$$\left| (I_1\, I_2\, J)\alpha F M \right\rangle = \sum_{F_i} c_{\alpha F_i}^{(F)} \left| (I_1\, J)\, I_2\, F_i\, F M \right\rangle \tag{8}$$

where the brackets around I_1 and J on the right-hand side of eq 8 indicate that they couple together prior to coupling to I_2. The energies of the hyperfine states needed in eq 6 are evaluated by forming the matrix elements of the

hyperfine Hamiltonian:

$$\langle (I_1 I_2 J)\ \alpha F M | H | (I_1 I_2 J)\ \alpha' F M \rangle = \sum_{F_i F_i'} c^{(F)}_{\alpha F_i} c^{(F)^*}_{\alpha' F_i'} \langle (I_1 J) I_2 F_i F M | H | (I_1 J) I_2 F_i' F M \rangle \qquad (9)$$

for which the matrix elements on the right-hand side can be calculated. Diagonalization of the Hamiltonian matrix in the hierarchical representation gives the energy eigenvalues, and the $c^{(F)}_{\alpha F_i}$ coefficients are obtained from the eigenvectors of the Hamiltonian matrix. Expressions for the matrix elements have been given by Altkorn et al.,[31] who considered the depolarization of aligned HF($v = 1, J$) prepared by one-photon absorption. For HCl, an additional term in the hyperfine Hamiltonian corresponding to the quadrupolar coupling of the nuclear spin of Cl, denoted by $\mathbf{I}_1$, to $\mathbf{J}$ must be considered. In a hierarchical-coupling scheme, the nuclear spin of the quadrupolar nucleus is assumed to couple to $\mathbf{J}$ to form the resultant $\mathbf{F}_i$. The necessary matrix elements are well known:[30]

$$\langle (I_1 J)\ I_2 F_i F M | H_Q | (I_1 J)\ I_2 F_i' F M \rangle = -\frac{1}{2} \mathrm{eq}Q \left[\frac{\frac{3}{4} C(C+1) - I_1(I_1+1) J(J+1)}{I_1 (2I_1 - 1)(2J-1)(2J+3)} \right] \delta_{F_i F_i'} \qquad (10)$$

where the quadrupolar term in the Hamiltonian is denoted by H_Q, eq$Q$ is the quadrupolar-coupling constant, and

$$C = F_i(F_i + 1) - J(J+1) - I_1(I_1 + 1) \qquad (11)$$

We illustrate the effect of hyperfine depolarization with calculations for HCl for which the H atom has a nuclear spin $I_H = 1/2$ and both isotopes of Cl have $I_{Cl} = 3/2$. We use a hyperfine Hamiltonian of the form presented by several authors.[44–46] Figure 2 shows the depolarization coefficients, $G^{(k)}(t)$, for $k = 2$ and $J = 1$ and 5 plotted against time. The quadrupolar coupling term in the Hamiltonian that arises from the quadrupolar moment of the Cl-atom nuclei causes the highest frequency oscillation and is thus responsible for most of the depolarization. Similar calculations for HF, with $I_F = 1/2$ (hence having no quadrupolar moment), show a much slower depolarization.[31–43] Note that as J increases, the effect of the depolarization becomes negligible.

Suppose that the reagent is prepared in its aligned state at $t = 0$ and the reaction products are probed at a later time, t. Then three regimes of hyperfine depolarization can be distinguished. If we ascribe a characteristic timescale to the hyperfine depolarization, denoted τ, which we define by

$$\frac{1}{\tau} = |E_{\alpha F} - E_{\alpha' F'}| / \hbar \qquad (12)$$

the regimes are:

1. $t \ll \tau$: the hyperfine depolarization can be neglected.
2. $t \gg \tau$: the hyperfine depolarization coefficient $G^k(t)$ can be replaced by an average depolarization coefficient, $\langle G^{(k)} \rangle$, as given in eqs 5 and 7.
3. $t \approx \tau$: in this range, the time dependence of the depolarization becomes significant.

In the regime of case (3), for an essentially instantaneous event that occurs at one well-defined initial time, the hyperfine depolarization can be calculated from eq 4 or 6. Such a situation occurs, for example, in optical pumping of molecules or photodissociation. For a reaction of a reagent aligned by optical pumping that is initiated at $t = 0$ and observed at a later time, $t = t'$, however, we must use a cumulative hyperfine-depolarization coefficient to describe the mean reagent alignment (neglecting the effects of collisional loss of alignment). This need for a cumulative coefficient arises because individual reaction events occur with equal probability throughout the time range (assuming no significant depletion of reagents), and reagents consumed at early times undergo hyperfine depolarization for a shorter time than those consumed at later times. We define the cumulative hyperfine-depolarization coefficient by

$$G^{(k)}_{\mathrm{cum}}(t') = \frac{1}{t'} \int_0^{t'} G^{(k)}(t)\, dt \qquad (13)$$

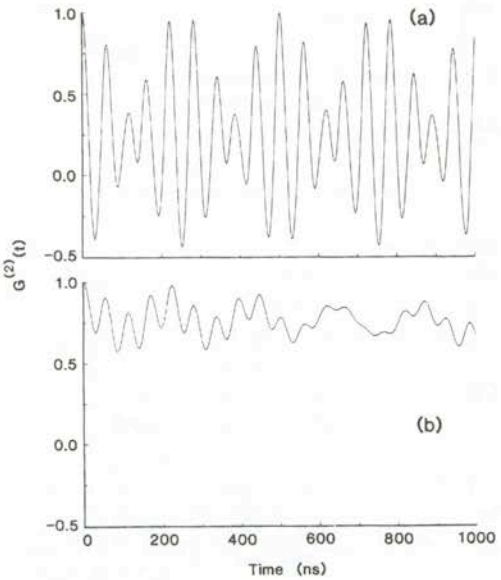

Fig. 2. Second-order hyperfine-depolarization coefficients for HCl($v = 1$) for (a) $J = 1$ and (b) $J = 5$ as a function of time, calculated from eq 6.

This cumulative depolarization coefficient is illustrated in Fig. 3 for HCl ($v = 1$) for $k = 2$ and $J = 1$ and 5.

For an electronic-ground-state molecule in a multiplet state, such as BaF($X^2\Sigma^+$), in which the spin is randomly polarized, we can account for the depolarization of the rotational angular momentum by the electronic spin, $\mathbf{S}_i$, in a similar way to the treatment of nuclear-hyperfine depolarization. If the spin is coupled to the internuclear axis [Hund's cases (a) and (c)], then the rotational angular momentum is not depolarized by $\mathbf{S}_i$. For Hund's case (b) coupling, with $\mathbf{N}_i$ denoting the total angular momentum except spin, we are interested in the moments of $\mathbf{N}_i$ rather than those of $\mathbf{J}_i$, which includes the spin, and we can combine the electronic-spin and hyperfine depolarizations in the same way as described above for two nuclear spins. Reid[35] has considered the consequences of spin depolarization in the context of photoelectron angular distributions from (1+1′) photoionization of NO via its $A^2\Sigma^+$ state.

4.2 Comparison with Experiment

In Fig. 4 we compare the ratio of the parallel to perpendicular intensity data from Fig. 1 with a calculation based on the hyperfine-depolarization analysis for HCl described in section 4.1. Intensity ratios were calculated from the time dependence of the HCl alignment using eqs 1, 3, and 6 and the analysis of Kummel et al.[40] for (2+1) REMPI probing of aligned ensembles to calculate the line-strength moments in eq 1. The calculated intensity ratios were convoluted with a 14-ns FWHM Gaussian that accounted for the time resolution of the experiment as described in section 2.

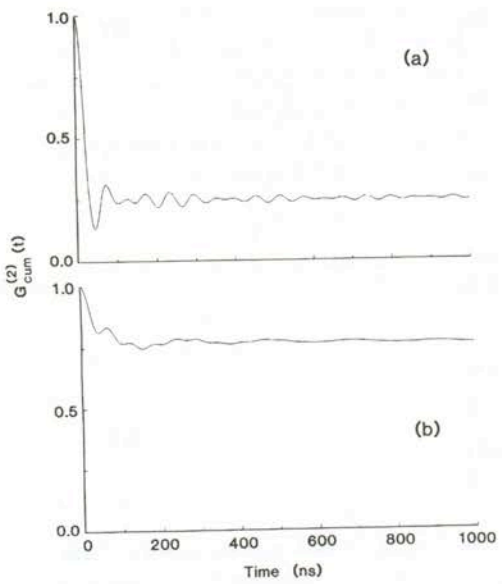

Fig. 3 The second-order cumulative hyperfine-depolarization coefficients for HCl($v = 1$) for (a) $J = 1$ and (b) $J = 5$ as a function of time, calculated from eq 13.

Our experimental scheme of IR excitation and REMPI detection is a novel method of studying quantum beats in the electronic ground state of a molecule. In this work, we are not concerned with the spectroscopy of the hyperfine sublevels of HCl($X^1\Sigma^+$), but our experimental method is very similar to that of Huber and coworkers,[38] who have studied Stark quantum beats in HC≡CCHO by IR absorption and UV laser-induced fluorescence (LIF).

4.3 Implications for Studies Using Aligned Reagents or Detecting Aligned Products

The calculations and experimental data presented in the preceding sections clearly show that hyperfine depolarization of aligned reagents prepared by optical excitation can be substantial for low values of the rotational quantum number, J. The depolarization can occur on a timescale comparable to or faster than the experimental pump/probe process. The consequences of hyperfine depolarization are much reduced for high values of J or for nuclei having small hyperfine splittings.

The use of aligned reagents in experimental studies of dynamical stereochemistry is expected to become more commonplace as the role of internal excitation of reagents on reactivity is more extensively investigated, and thus optical-excitation techniques are more widely used

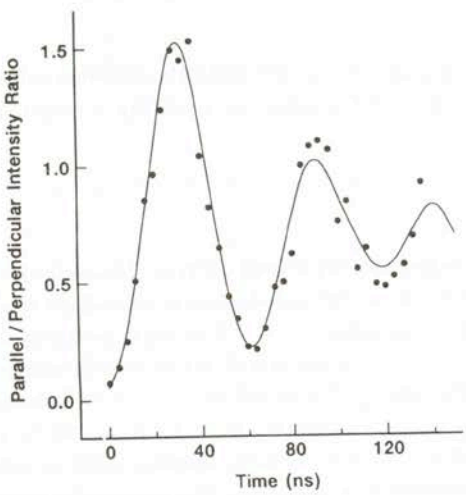

Fig. 4. The ratio of the ion signals detected with the UV probe beam polarized parallel and perpendicular to the polarization vector of the IR excitation beam plotted as a function of the time delay between the excitation and probe pulses. The experimental points (dots) are the ratio of the data sets (c) and (b) shown in Fig. 1. HCl($v = 1$, $J = 1$) is prepared rotationally aligned by one-photon absorption using a linearly polarized IR beam. The probe laser is of fixed, linear polarization and is tuned to the R(1) line of the HCl $F^1\Delta$-$X^1\Sigma^+$(0,1) transition. The theoretical curve (solid line) is generated by convoluting the results of eqs 1, 3, and 6 with a 14-ns Gaussian function that describes the time resolution of the experiment.

for reagent state preparation. Novel methods employed in this laboratory to study reaction differential cross sections[39, 47, 48] and reagent and product alignment effects[13] allow much of the alignment in the frame of $\mathbf{E}_{JR}$ to survive into the collision frame (the frame of the reagent relative velocity). A principal concern that remains, however, is the depolarization of this reagent alignment by hyperfine or spin coupling (and likewise, the depolarization of reaction-product alignment). We have shown that for HCl in rotational states with small values of J, this depolarization must be taken into account in alignment studies. For example, for HCl($v = 1$, $J = 1$) used as an aligned reagent, the extent of depolarization of the quadrupolar alignment after a delay of only 100 ns is approximately 75%. The extent of hyperfine depolarization is markedly reduced for larger values of J; for $J = 5$, the maximum depolarization is of the order of 25%. The use of seeded, pulsed expansions of reagents to limit collision energy uncertainties,[13,39,47] however, places restrictions on the values of the rotational quantum number of the excited state that can be accessed by one-photon excitation because of rotational cooling in the expansion. The consequences of using thermal rather than translationally cooled reagents are twofold: first, a large uncertainty exists in the reagent collision energies, particularly for hot-atom reactions,[49] and second, the thermal motion of the reagents reduces the effective alignment in the collision frame.[23]

Thus, the choice of experimental conditions requires a balance to be struck between the need for high rotational angular momentum to reduce alignment depolarization and the need to restrict thermal blurring of collision energies and collision-frame alignment. This compromise is likely to require an assessment of the importance of hyperfine depolarization; i.e., the depolarization of orientation and alignment by the presence of nonzero nuclear spins is perilous to ignore. As described for HCl($v = 1$, $J = 1$), its inclusion, however, is easy to carry out by evaluating the cumulative hyperfine-depolarization coefficient.

CONCLUSIONS

The use of HCl as an aligned reagent in studies of dynamical stereochemistry is strongly limited by the effects of hyperfine depolarization of the rotational alignment for low rotational quantum numbers. The quadrupolar contribution of the chlorine-atom nuclear-spin coupling with the rotational angular momentum of the HCl results in a depolarization on a timescale of the order of 20 ns. The resultant loss of reagent alignment can be reduced by preparing HCl in higher rotational quantum states, but then pulsed expansions of the reagents cannot be employed, and as a result, bulb experiments will suffer from a large uncertainty in reagent collision energies caused by the thermal motion of the reagents. Even for low values of J, however, hyperfine depolarization does not destroy reagent alignment completely, and if an experiment can be designed to be highly sensitive to reagent alignment, the effects of dynamical stereochemistry on state-resolved integral cross sections and other observables might still be apparent. The alternative approach of conducting experiments at very short time delays between initiation and detection (time intervals of less than 20 ns in this instance) is generally not feasible because insufficient time exists for the build-up of reaction products.

Acknowledgments. WRS thanks the NSF for a predoctoral fellowship. This work was supported by the National Science Foundation under grant number CHE 89-21198.

REFERENCES

(1) Zare, R. N. *Ber. Bunsenges. Phys. Chem.* 1982, **86**: 422.
(2) Parker, D. H.; Bernstein, R. B. *Annu. Rev. Phys. Chem.* 1989, **40**: 561.
(3) Harland, P.W.; Carman, H.S.; Phillips, L.F.; Brooks, P.R. *J. Chem. Phys.* 1990, **93**: 1089.
(4) Brooks, P.R.; Harland, P.W.; Phillips, L.F.; Carman, H.S. *J. Phys. Chem.* 1992, **96**: 1557.
(5) Loesch, H.J.; Remscheid, A. *J. Chem. Phys.* 1990, **93**: 4779.
(6) Loesch, H.J.; Stenzel, E.; Wustenbecker, B. *J. Chem. Phys.* 1991, **95**: 3841.
(7) Loesch, H.J.; Stienkemeier, F. *J. Chem. Phys.* 1993, **98**: 9571.
(8) Janssen, M.H.M.; Parker, D. H.; Stolte, S. *J. Phys. Chem.* 1991, **95**: 8142.
(9) Buelow, S.; Radhakrishnan, G.; Catanzarite, J.; Wittig, C. *J. Chem. Phys.* 1985, **83**: 444.
(10) Chen, Y.; Hoffmann, G.; Oh, D.; Wittig, C. *Chem. Phys. Lett.* 1989, **159**: 426.
(11) Soep, B.; Whitham, C.J.; Keller, A.; Visticot, J.P. *Faraday Discuss. Chem. Soc.* 1991, **91**: 191.
(12) Scherer, N.F.; Khundkar, L.B.; Bernstein, R.B.; Zewail, A.H. *J. Chem. Phys.* 1987, **87**: 1451.
(13) Orr-Ewing, A.J.; Zare, R. N. In *Chemical Dynamics and Kinetics of Small Free Radicals*; Liu, K.; Wagner, A., Eds.; World Scientific: Singapore, in press.
(14) Bergmann, K. In *Atomic and Molecular Beam Methods. Volume 1.*; Scoles, G., Ed.; Oxford University Press: New York, 1988, p. 293.
(15) Broyer, M.; Gouedard, G.; Lehmann, J.C.; Vigué, J. *Adv. At. Mol. Phys.* 1976, **12**: 165.
(16) Booth, J.P.; Bragg, S.L.; Hancock, G. *Chem. Phys. Lett.* 1985, **113**: 509.
(17) Kessler, W.J.; Poliakoff, E.D. *J. Chem. Phys.* 1986, **84**: 3647.
(18) Dubs, R.L.; McKoy, V.; Dixit, S.N. *J. Chem. Phys.* 1988,

88: 968.
(19) Dubs, R.L.; McKoy, V. *J. Chem. Phys.* 1989, **91**: 5208.
(20) McCormack, E.F.; Pratt, S.T.; Dehmer, J.L.; Dehmer, P.M. *J. Chem. Phys.* 1990, **92**: 4734.
(21) Karny, Z.; Estler, R.C.; Zare, R.N. *J. Chem. Phys.* 1978, **69**: 5199.
(22) McKendrick, K.G. *J. Chem. Soc., Faraday Trans. 2*, 1989, **85**: 1255.
(23) Kettleborough, J.A.; McKendrick, K. G. *J. Phys. Chem.* 1991, **95**: 8255.
(24) Pibel, C.D.; Moore, C.B. *J. Chem. Phys.* 1990, **93**: 4808.
(25) Sitz, G.O.; Farrow, R.L. *Proceedings of 12th Combustion Research Conference, Office of Basic Energy Sciences, U.S. Department of Energy.* Tahoe City, CA. 1990, p. 79.
(26) Dopheide, R.; Zacharias, H. *J. Chem. Phys.* 1993, **99**: 4864.
(27) Madden, P.A. *Chem. Phys. Lett.* 1975, **35**: 521.
(28) Fano, U.; Macek, J.H. *Rev. Mod. Phys.* 1973, **45**: 553.
(29) Blum, K. *Density Matrix Theory and Applications.* Plenum Press: New York, 1981.
(30) Zare, R.N. *Angular Momentum. Understanding Spatial Aspects in Chemistry and Physics.* Wiley Interscience: New York, 1988.
(31) Altkorn, R.; Zare, R.N.; Greene, C.H. *Mol. Phys.* 1985, **55**: 1.
(32) Yan, C.; Kummel, A.C. *J. Chem. Phys.* 1993, **98**: 6869.
(33) Strand, M.P.; Hansen, J.; Chien, R.-L.; Berry, R. S. *Chem. Phys. Lett.* 1978, **59**: 205.
(34) Chien, R.-L.; Mullins, O.C.; Berry, R.S. *Phys. Rev. A*, 1983, **28**: 28.
(35) Reid, K.L. *Chem. Phys. Lett.* 1993, **215**: 25.
(36) Felker, P.M.; Zewail, A.H. *Adv. Chem. Phys.* 1988, **70**: 265.
(37) Hack, E.; Huber, J.R. *Int. Rev. Phys. Chem.* 1991, **10**: 287.
(38) Walther, T.; Bitto, H.; Huber, J.R. *Chem. Phys. Lett.* 1993, **209**: 455.
(39) Simpson, W.R.; Orr-Ewing, A.J.; Zare, R.N. *Chem. Phys. Lett.* 1993, **212**: 163.
(40) Kummel, A.C.; Sitz, G.O.; Zare, R.N. *J. Chem. Phys.* 1986, **85**: 6874.
(41) Herzberg, G. *Atomic Spectra and Atomic Structure.* Dover: New York, 1945.
(42) Flynn, G.W.; Weston, R.E. *Annu. Rev. Phys. Chem.* 1986, **37**: 551.
(43) Altkorn, R. Ph.D. Thesis, Stanford Univ., Stanford, CA, 1984.
(44) Kaiser, E. W. *J. Chem. Phys.* 1969, **53**: 1686.
(45) Code, R.F.; Khosla, A.; Ozier, I.; Ramsey, N.F.; Yi, P.N. *J. Chem. Phys.* 1968, **49**: 1895.
(46) Muenter, J.S.; Klemperer, W. *J. Chem. Phys.* 1970, **52**: 6033.
(47) Shafer, N.E.; Orr-Ewing, A.J.; Simpson, W.R.; Xu, H.; Zare, R.N. *Chem. Phys. Lett.* 1993, **212**: 155.
(48) Shafer, N.E.; Xu, H.; Tuckett, R.P.; Springer, M.; Zare, R.N. *J. Phys. Chem.* 1994, **98**: 3369.
(49) van der Zande, W.; Zhang, R.; McKendrick, K.G.; Zare, R.N.; Valentini, J. J. *J. Phys. Chem.* 1991, **95**: 8205.